SUPPORTING INFORMATION

Sepiolite as a Novel Polysulfide Trapper for energy applications: an electrochemical, X-ray spectroscopic and DFT study

Francisco García-Soriano[a,b,e*], Sergio Andrés Ceppi[a,b], Fernando Pablo Cometto[c,d], Emiliano Nicolás Primo[a,b], Daniel Eugenio Barraco[a,b], Ezequiel Pedro Marcos Leiva[c,e], Guillermina Leticia Luque[c,e], Guillermo Stutz[a,b], German Lener[c,e*], María Victoria Bracamonte [a,b,e*]

[a]Instituto de Física Enrique Gaviola, IFEG, Consejo Nacional de Investigaciones Científicas y Técnicas de la República Argentina, Av. Haya de la Torre esq. Medina Allende, Córdoba, Argentina.

[b]Facultad de Matemática, Astronomía Física y Computación, Universidad Nacional de Córdoba, Av. Haya de la Torre esq. Medina Allende, Córdoba, Argentina.

[c]Instituto de Investigaciones en Fisicoquímica de Córdoba, INFIQC, Consejo Nacional de Investigaciones Científicas y Técnicas de la República Argentina (CONICET), Av. Haya de la Torre esq. Medina Allende, Ciudad Universitaria, 5000 Córdoba, Argentina

[d]Departamento de Fisicoquímica, Facultad de Ciencias Químicas, Universidad Nacional de Córdoba, Ciudad Universitaria, 5000 Córdoba, Argentina.

[e]Departamento de Química Teórica y Computacional, Facultad de Ciencias Químicas, Universidad Nacional de Córdoba, Ciudad Universitaria, 5000 Córdoba, Argentina.
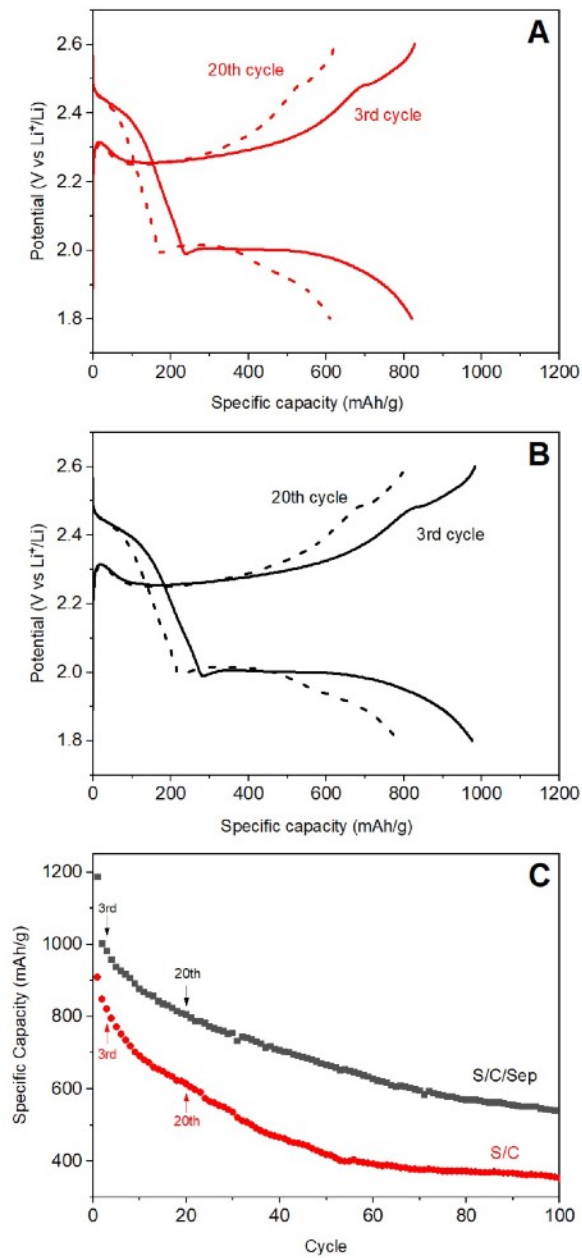
Figure S1. Charge/Discharge profiles for S/C **(A)** and S/C/Sep **(B)** cathodes and cycle stability of Li-S cells prepared with S/C (red) and S/C/Sep (black) cathodes **(C)**.

		S/C						S/C/SEP					
		Lithiated			Delithiated			Lithiated			Delithiated		
		BE, eV	FWHM	%At	BE, eV	FWHM	%At	BE, eV	FWHM	%At	BE, eV	FWHM	%At
S2p*	S1	160.8	1.16	2.02				160.8	1.25	0.18	160.8		
	S2	162.3	1.16	0.87	162.3	1.35	0.62	162.3	1.25	0.89	162.3	1.40	0.77
	S3	164.0	1.40	0.40	164.0	1.35	1.84	164.0	1.25	0.63	164.0	1.10	0.52
	S4							166.8	1.20	0.13	166.8	1.60	0.69
	S5	167.5	1.16	0.04	167.5	1.40	0.39	167.5	1.20	0.22	167.5	1.30	1.91
	S6				169.5	1.35	0.06	169.5	1.20	0.08	169.5	1.30	0.52
	Total			3.34			2.91			2.13			4.41
C1s	C1	284.4	1.30	9.72	284.4	1.25	8.77	284.4	1.0	7.58	284.4	1.0	6.98
	C2	284.8	1.20	17.36	284.8	1.20	19.49	284.8	1.0	19.95	284.8	1.0	13.71
	C3-C3'	285.7	1.10	1.22	285.7	1.10	0.97	285.7	1.0	2.39	285.7	1.0	3.80
	C4	286.3	1.30	15.45	286.3	1.41	13.25	286.3	1.24	5.99	286.3	1.24	8.00
	C5	288.5	1.35	1.91	288.5	1.41	3.90	288.5	1.0	2.20	288.8	1.0	3.54
	C6	290.1	1.30	0.17	290.1	1.41	2.92	289.8	1.41	6.19	289.9	1.41	6.98
	Total			45.83			49.30			44.30			43.01
O1s	O1	528.0	1.40	0.75									
	O2	530.6	1.60	4.26	530.5	1.40	4.38						
	O3-O3'	531.6	1.40	6.28	531.5	1.60	8.11	531.2	1.60	23.33	531.2	1.60	25.78
	O4-O4'	533.0	1.60	7.47	533.0	2.00	9.32	532.5	1.70	5.37	532.5	1.70	7.22
	Total			18.76			21.81			28.70			33.00

Table S1. XPS data showing the individual percentages of each atom on its different chemical environment obtained from the best fitting procedure of spectra shown in Figures 2, S1 and S2 for cathodes lithiated and delithiated on the 20th cycle.

XPS C1s analysis

From the analysis of C1s spectra, 6 different components can be distinguished: **C1** at 284.4 eV, attributed to sp^2 carbon atoms from C super P in the slurry, **C2** at 284.8 eV to C-H/C-C and adventitious carbon atoms, C3 at 285.7 eV to C-O in defected sp^2 C and C atoms from $COSO_2^{2-}$ (the last one only present in samples with SEP), **C4** at 286.3 eV related to C-O that belongs to remaining electrolyte (TEGDME) solvent and **C6** and **C5** components assigned to C-F species derived from PVDF and decomposed PVDF, respectively (Fig. S1 and Table S1). In both lithiated and delithiated cathodes no significant changes are observed for the signals associated with the electrolyte, the binder, or the C-C bond for both electrodes. The only minor difference noted corresponds to the feature assigned to **C4** feature. In the cathodes without SEP this component represents almost the 30% of the total amount of C atoms, whereas only represents the 15% with samples with SEP (Table S1).
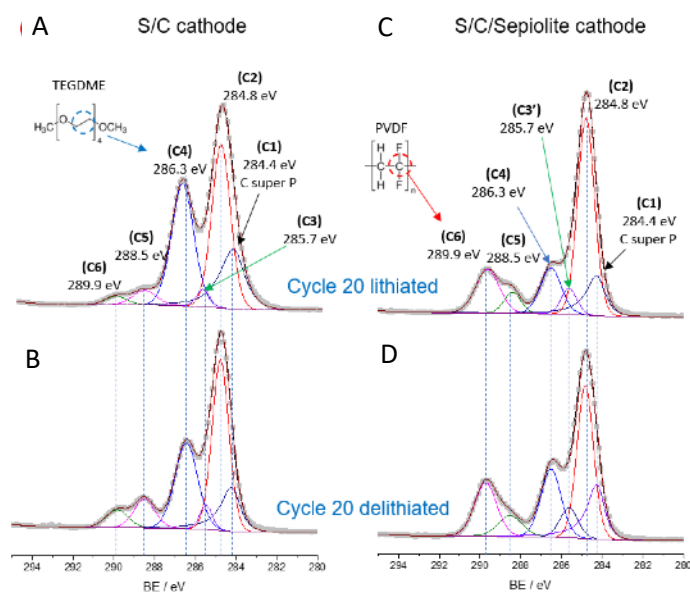
Figure S2. C1s spectra of S/C cathodes without (a, b) and with SEP (c, d) as an additive after 20 cycles.

XPS O1s analysis

The analysis of O1s spectra is not straightforward. It is well known that this region (530–534 eV) is congested with signals originating from organic containing oxygen atoms, hydroxyls, and water molecules in most cases (REF). In the case of these samples, a wide range of oxygenated species could be present in the cathode: decomposed solvent and electrolyte, nitrates, S-O species, metal oxides (such as Li_2O), traces of water, etc. Within this context (and the conditions that measurements were performed), it is therefore unlikely to make a single assignment of each peak. Therefore, the assignment of each peak, obtained by a conservative fitting procedure, could involve more than one specie. Fig. S2 (and Table S1), shows that 4 peaks can be distinguished for samples without SEP and only 2 for samples with SEP. In the fully lithiated S/C cathode, **O1** component at 528.0 eV is attributed to Li_2O, whereas components **O2**, **O3** and **O4** to the presence of C=O, C-OH and O-C-O (from TEGDME) + nitrates + sulfites/sulfates, respectively. As we suggested above, the assignment of only 2 peaks for SEP-cathodes does not imply that only 2 different species are present in this sample. On the contrary, the same species as in S/C can be present and another important signal (531.2 eV) that evolves the rest of the signals. According to bibliography (REF), this component (**O3'**) could be attributed to -OH interactions around SEP additive. To emphasize this hypothesis, the analysis of all the possible O-containing species can be made from the total relative percentage of atoms bond to O atoms. For example, N atoms is bond to 3 O atoms (NO_3^-), S bond to 2 (**S4**), 3 (**S5**) and 4 (**S6**) O atoms, C bond to 1 O atom (**C3**, **C4**) and Li with 2 O atoms. From this analysis, it is possible to obtain an excess of O atoms that are not bond to C, S, Li and N. As expected, no excess of O atoms was obtained for S/C cathodes and an excess of 17% and 11% for samples with SEP lithiated and delithiated, respectively. The difference between SEP samples (lithiated vs. delithiated) arises from the amount of oxidized S species in delithiated samples.
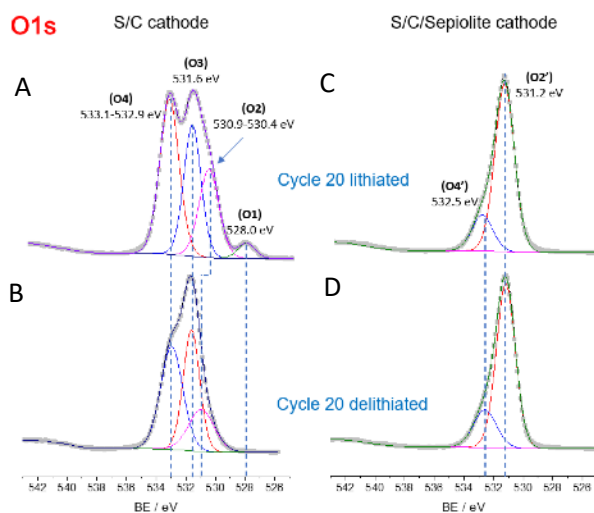
Figure S3. O1s spectra of S/C cathodes without (a, b) and with sepiolite (c, d) as an additive after 20 cycles.
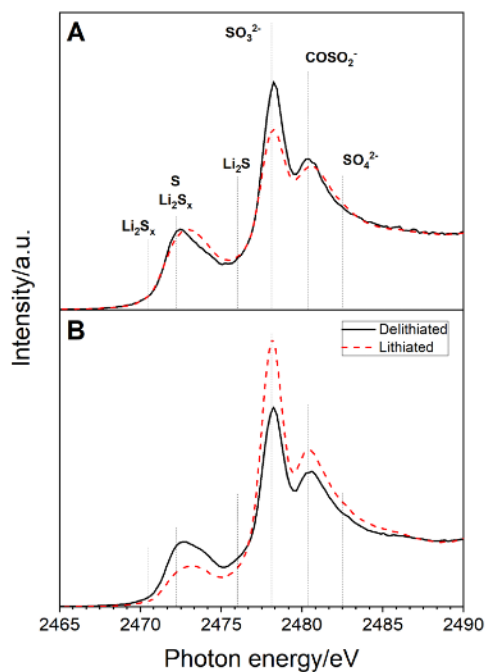

Figure S4. S K-edge XANES measurements in fluorescence mode of celgard separators used in cells without (a) and with sepiolite (b) as an additive after 20 cycles.

DFT Calculations

To model the sepiolite material we use the published crystallographic file in 10.1127/0935-1221/2011/0023-2105 (www.crystallography.net/cod/cif/9/01/57/9015793.cif) as starting input. That model corresponds to a bulk material with water molecules inside the pores:
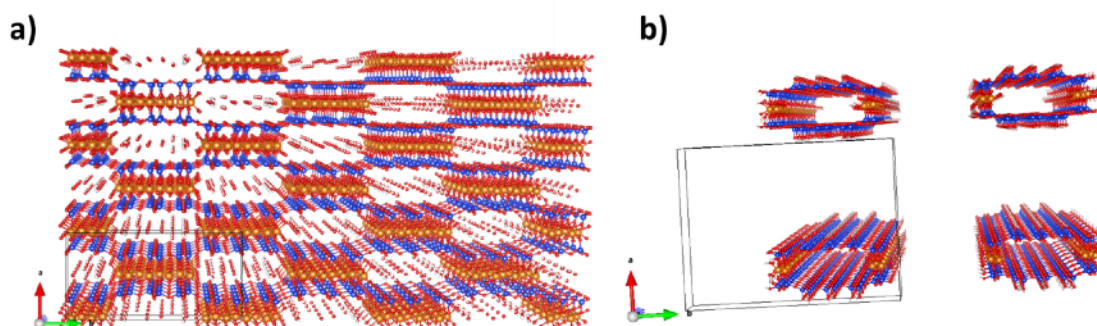
Figure S5. a) Model of sepiolite based on 10.1127/0935-1221/2011/0023-2105. b) final pore structure built for Li_2S_6 adsorption.

The bulk structure was refined through optimization employing the Conjugate Gradient (CG) algorithm, employing variable unit cells. As depicted in Figure S5a, the unit cell does not inherently depict the pore. Consequently, we proceeded to adapt the unit cell to accurately depict the pore. Thus, once the bulk converged the bulk structure, the pore structure was built by elongation of the *x* and the *y* axis remaining the periodicity along the z axis, modeling a unidimensional pore. Since some -Si-O-X bonds were cleaved the unsaturated electronic density was fixed by adding of H atoms, generating -SiOH, which is reasonable in silica based surfaces (Carraro et al. 2016). Moreover, according to the bibliography, the external channels of sepiolite are formed by those functional groups (Volle et al. 2012). Although water molecules in the pore were removed at the beginning, the starting model includes Mg-OH groups inside the pore. In order to evaluate the stability of these OH sites, ab-initio molecular dynamic simulation (MDS) in Born-Oppenheimer scheme at 300 K were performed. As a result, we found that Mg-OH groups break away in a few picoseconds, placing the OH into the pore (fig S6).
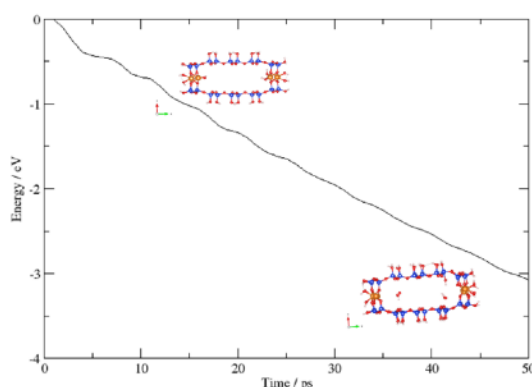

Figure S6. Profile of energy vs. time of sepiolite pore structure in Born-Oppenheimer Molecular Dynamic.

Thus, the representation of the sepiolite is a nanotube with 194 atoms. Since the K-point representation is 1x1x2 in a 1x1x3 supercell, the system consists of 582 atoms, 6510 orbitals and 8388 projectors. Thus, this simulation addresses the thermochemistry of the adsorption of Li_2S_6 in two types of sites, inside and outside the pore in a relatively big system. The outside site was built to represent the external channels that are present in sepiolite (Volle et al. 2012).

References

Carraro, P.M. et al. 2016. «Understanding the Role of Nickel on the Hydrogen Storage Capacity of Ni/MCM-41 Materials». *Microporous and Mesoporous Materials* 231: 31-39.

Volle, Nicolas et al. 2012. «Controlled Interactions between Silanol Groups at the Surface of Sepiolite and an Acrylate Matrix: Consequences on the Thermal and Mechanical Properties». *Materials Chemistry and Physics* 134(1): 417-24.